Crystallization in Two-Component Coulomb Systems

M. Bonitz,[1] V. S. Filinov,[1,2] V. E. Fortov,[2] P. R. Levashov,[2] and H. Fehske[3]

[1]*Institut für Theoretische Physik und Astrophysik, Christian-Albrechts-Universität zu Kiel, Leibnizstrasse 15, 24098 Kiel, Germany*
[2]*Institute for High Energy Density, Russian Academy of Sciences, Izhorskay 13/19, Moscow 127412, Russia*
[3]*Institut für Physik, Ernst-Moritz-Arndt-Universität Greifswald, Domstrasse 10a, D-17489 Greifswald, Germany*
(Received 21 July 2005; published 2 December 2005)

The analysis of Coulomb crystallization is extended from one-component to two-component plasmas. Critical parameters for the existence of Coulomb crystals are derived for both classical and quantum crystals. In the latter case, a critical mass ratio of the two charged components is found, which is of the order of 80. Thus, holes in semiconductors with sufficiently flat valence bands are predicted to spontaneously order into a regular lattice. Such hole crystals are intimately related to ion Coulomb crystals in white dwarf and neutron stars as well as to ion crystals produced in the laboratory. A unified phase diagram of two-component Coulomb crystals is presented and is verified by first-principles computer simulations.

PACS numbers: 52.27.−h, 52.25.−b

Crystallization is one of the most fundamental many-particle phenomena in charged particle systems. After the prediction of a highly correlated state of the electron gas—the electron Wigner crystal [1]—there has been an active search for this phenomenon in many fields. Crystallization of electrons was observed on the surface of helium droplets [2] and is predicted to occur in semiconductor quantum dots [3]. Moreover, crystals of ions have been observed in traps [4] and storage rings [5] and are expected to occur in layered systems [6]. The necessary condition for the existence of a crystal in these one-component plasmas (OCPs) is that the mean Coulomb interaction energy $e^2/\bar{r}$ ($\bar{r}$ denotes the mean interparticle distance) exceeds the mean kinetic energy (thermal energy $\frac{3}{2}k_B T$ or Fermi energy E_F in classical or quantum plasmas, respectively) by a factor Γ larger than Γ^{cr}, which in a classical OCP is given by 175 [2,7]. In a quantum OCP at zero temperature, the coupling strength is measured by the Brueckner parameter $r_s \equiv \bar{r}/a_B$ (a_B denotes the effective Bohr radius) with a critical value for crystallization of $r_s^{cr} \approx 100$ (160) for fermions (bosons) [8].

The vast majority of Coulomb matter in the Universe, however, exists in the form of *neutral plasmas*, containing (at least) two oppositely charged components [two-component plasma (TCP)]. Coulomb crystallization in a TCP has been observed as well, e.g., in colloidal and dusty plasmas [9,10], and it is predicted to be possible in laser-cooled expanding plasmas [11]. The lattice of heavy particles is immersed into a structureless gas of the light component which does not affect the former. Besides these *classical TCP crystals,* it is expected that, in the interior of white dwarf stars and in the crust of neutron stars, there exists an entirely different type of TCP crystals [12]: crystals of bare nuclei (e.g., fully ionized carbon, oxygen, iron) which are embedded into an extremely dense degenerate Fermi gas of electrons. No such *quantum TCP crystals* have been observed in the laboratory, despite early suggestions [13]. It is an open question what classical and

quantum TCP crystals (being separated by 15–20 orders of magnitude in density) have in common and if there exists an integrative phase diagram.

This Letter aims to answer these questions. We show that, in fact, a common phase diagram of Coulomb crystals in a generic neutral TCP (consisting of electrons and point-like ions [14]) exists which is governed by five parameters—density and temperature (as in the OCP case) and, additionally, by the asymmetry of the heavy (h) and electron (e) components with respect to three fundamental properties: mass, charge, and temperature, $M = m_h/m_e$, $Z = Z_h/Z_e$, and $\Theta = T_e/T_h$, respectively. We show that classical TCP crystals require a critical charge ratio Z, whereas quantum TCP crystals exist only if the mass ratio M exceeds a critical value of about 80. As a consequence, we predict the existence of quantum TCP crystals of protons in a dense hydrogen plasma and crystals of holes in semiconductors.

Let us consider a locally neutral system of electrons and Z-fold charged heavy particles. The stationary state of the TCP is characterized by the dimensionless electron temperature $T_e = 3k_B T/2E_B$ and mean interelectron distance $r_{se} = \bar{r}_e/a_B$, where E_B denotes the *e-h* binding energy, and the dimensionless density is given by $na_B^3 = 3/(4\pi r_{se}^3)$.

Classical crystal.—For the existence of a Coulomb crystal in the presence of a classical gas of electrons, we first require that the heavy component is able to form a classical OCP crystal, i.e.,

$$\Gamma_h \geq \Gamma^{cr}, \tag{1}$$

and, second, that the electrons do not destroy that crystal, e.g., as a result of screening of the heavy particle interaction. However, the main obstacle for the crystal turns out to be the formation of *e-h* bound states (atoms, excitons, etc.) because this drastically reduces the *h-h* correlation energy causing violation of condition (1). Therefore, we require that no significant fraction of heavy particles is trapped in Coulomb bound states, for which a conservative estimate is

given by $T_e \gtrsim 1$, stating that the electrons have sufficiently high kinetic energy to escape the binding potential V_{eh}. Making use of charge neutrality, $n_e = n_h Z$, and the definitions of Γ and T_e, we find from Eq. (1) that the classical TCP Coulomb crystal exists between the temperatures $T_e^{(1)}$ and $T_e^{(2)}$, given by

$$T_e^{(1)} \approx 1 \quad \text{and} \quad T_e^{(2)}(r_{se}) = \frac{3\Theta Z^{2/3}}{\Gamma^{cr}} \frac{1}{r_{se}}, \qquad (2)$$

and only if the ion charge exceeds a critical value $Z^{cr}(\Theta, r_{se}) = (\Gamma^{cr} r_{se}/3\Theta)^{3/2}$, which is independent of the mass ratio M.

Quantum TCP crystal and critical mass ratio.—In the presence of quantum electrons, the condition for crystallization of the heavy particles follows from the quantum OCP result, $r_{sh} \geq r_s^{cr}$. To be specific, we will concentrate on hydrogenlike Coulomb bound states, where $E_B = Ze^2/(8\pi\epsilon_0\epsilon_r a_B)$ and $a_B = \hbar^2 4\pi\epsilon_0\epsilon_r/(m_r Ze^2)$ [ϵ_r and m_r are the background dielectric constant and the reduced mass $m_r^{-1} = m_h^{-1}(1 + M)$]. Since r_s^{cr} refers to the critical interparticle distance in units of the hydrogenic a_B^H [8], we first transform to the relevant effective Bohr radius a_B. Further, we eliminate r_{sh} by expressing $\bar{r}_h$ by $\bar{r}_e$ again using charge neutrality. Then the OCP result can be rewritten as

$$Z^{4/3}(M + 1)r_{se} \geq r_s^{cr}. \qquad (3)$$

This crystal of heavy particles will survive in the presence of electrons only if, as in the classical case, bound states are unstable, which, at zero temperature, occurs due to pressure ionization at densities above the Mott density, i.e., $r_{se} \leq r_s^{Mott} \approx 1.2$ (see below). With increasing temperature, ionization becomes possible at lower density which we indicate by a monotonically decreasing function $1/r_s^{Mott}(T_e)$, which vanishes when $T_e \to 1$ because thermal ionization prevails. Combination of (3) with the existence of pressure ionization allows us to eliminate r_{se}, yielding the criterion for the existence of a TCP crystal in the presence of a neutralizing background of quantum electrons as

$$M \geq M^{cr}(Z, T_e) = \frac{r_s^{cr}}{Z^{4/3} r_s^{Mott}(T_e)} - 1, \qquad (4)$$

which exists in a finite electron density range between

$$n^{(1)}(T_e) = \frac{3}{4\pi}\left[\frac{1}{r_s^{Mott}(T_e)}\right]^3, \qquad n^{(2)}(T_e) = n^{(1)}(T_e)K^3,$$
$$K = (M + 1)/(M^{cr} + 1), \qquad (5)$$

and below a critical temperature T^*. The density limits follow from the Mott criterion and from Eq. (3), whereas T^* is estimated [3] by the crossing point of the classical and quantum asymptotics of an OCP crystal (1) and (3)

$$T^* = 6\frac{Z^2\Theta(M + 1)}{\Gamma^{cr}r_s^{cr}}. \qquad (6)$$

In absolute units, the density interval scales as Z^3 and the critical temperature as $M \cdot Z^4 \cdot \Theta$. The critical mass ratio for singly charged ions in an isothermal TCP ($\Theta = 1$) equals 83 (132) for fermions (bosons) and decreases with increasing temperature (due to the lower Mott density) and with increasing Z.

Examples ($\Theta = 1$).—(i) For a crystal of $C^{6+}[O^{8+}]$ nuclei expected to exist in the interior of white dwarf stars, the minimum density is given by $n_e^{(1)}(0) = 2 \times 10^{26}$ cm^{-3} [6.6×10^{26} cm^{-3}] and $T^* = 10^9$ K [4.2×10^9 K] [15]. (ii) Hydrogen and helium are predicted to form crystals as well: A crystal of protons [α particles] is stable between $n_e^{(1)}(0) = 0.9 \times 10^{24}$ cm^{-3} [7.5×10^{24} cm^{-3}] and $n_e^{(2)}(0) = 10^{28}$cm^{-3} [1.3×10^{30} cm^{-3}] and below $T^* = 6.6 \times 10^4$ K [4.2×10^6 K] and should be achievable in laboratory experiments with laser or ion beam compression techniques. (iii) Crystallization of holes in semiconductors ($Z = 1$) is predicted for materials with a hole to electron mass ratio $M \geq M^{cr} \approx 83$ [16]. This value is feasible in intermediate valence semiconductors, such as Tm[Se, Te] [17]. For example, for $M = 100$ (using $\epsilon_r = 20$), the parameters are $n_e^{(1)}(0) = 1.2 \times 10^{20}$ cm^{-3}, $n_e^{(2)}(0) = 2.1 \times 10^{20}$ cm^{-3}, and $T^* \approx 9$ K.

Numerical verification.—Of course, the boundary of the TCP crystal phase at low densities contains some uncertainty, due to the very complex transition from an atomic system to a Coulomb crystal of heavy particles embedded into delocalized electrons. This transition, which extends over a finite density interval, may involve liquidlike behavior, clusters, and, at low temperature, phase separation, an analysis of which is beyond the present study. We estimate that these effects give rise to an uncertainty of the minimum density (Mott density) $n^{(1)}$ of the order of 30%. Further, the error of r_s^{cr} is about 20% [8]; thus, the critical parameters carry an uncertainty of about 50%. For particular systems, more accurate predictions are possible if the Mott parameter r_s^{Mott} is known, e.g., from computer simulations. Note that the complex processes of interest pose an extreme challenge to the simulations: They must self-consistently include the full Coulomb interactions, *e-h* bound state formation in the presence of a surrounding plasma, pressure ionization, and the quantum and spin properties of the light and heavy species.

We, therefore, have performed extensive direct fermionic path integral Monte Carlo (PIMC) simulations of electron-hole plasmas which are based on our previous results for dense hydrogen-helium plasmas [18], *e-h* plasmas [19], and electron Wigner crystallization [3]. While the so-called sign problem prohibits PIMC simulations of the ground state of a fermion system, here we restrict ourselves to temperatures at the upper boundary of the hole crystal phase, i.e., $T_e = 0.06$–0.2. Studying mass ratios in the range of $M = 1$–2000 and densities corresponding to $r_{se} = 0.6$–13, the simulations cover a large variety of Coulomb systems—from positronium, over typical semiconductors, to hydrogen. We start with the

case of low densities (large r_{se}) to determine the Mott density $n^{(1)}$. Here the TCP consists of excitons and biexcitons, and we found [20] that for $r_{se} \leq 1.2$ less than 10% of the electrons and holes are bound, approving the choice of r_s^{Mott} made above. Thus, crystallization should become possible. This is confirmed by our simulations (see Figs. 1 and 2) showing results for $r_{se} = 0.63$ and different mass ratios M. Figure 1 displays snapshots of the e-h system in the simulation box. In all figure parts, the electrons form a nearly homogeneous Fermi gas—individual electrons penetrate each other, extending far beyond the main simulation cell (shown by the gray grid lines). At the same time, the hole arrangement changes dramatically. While, at $M = 5$, the holes are in a gaslike state (similar to the electrons), at $M = 50$ their structure resembles a liquid and, at $M = 100$ and 800, they are periodically arranged in space. Thus, between $M = 100$ and 50, the holes crystallize. The figure also clearly shows the mechanism of the quantum melting process: With reduction of M, the individual hole wave functions grow continuously until, at $M = M^{cr}$, they exceed a critical size which allows for tunneling between lattice sites, giving rise to hole delocalization, i.e., crystal melting. Vice versa, increase of M reduces the spatial extension of each hole which stabilizes the crystal (at $M = 800$, they shrink to a dot; see Fig. 1).

The crystallization transition is further supported by the behavior of the pair distribution functions g_{ab}, shown in Fig. 2. At $M \leq 50$ (upper two panels), the h-h functions (solid black curves) have only a single peak like in a liquid. However, for $M = 100$, g_{hh} exhibits periodic oscillations with a deep first minimum, typical for a crystal. The crystal exists only at low temperature; an increase of T by a factor of 2 (from the lower right figure to the lower left) causes thermal melting. Further, the e-e and e-h pair distributions allow us to understand the behavior of the electrons: In the hole crystal phase, the electrons exhibit periodic density modulations, indicating the formation of Bloch waves
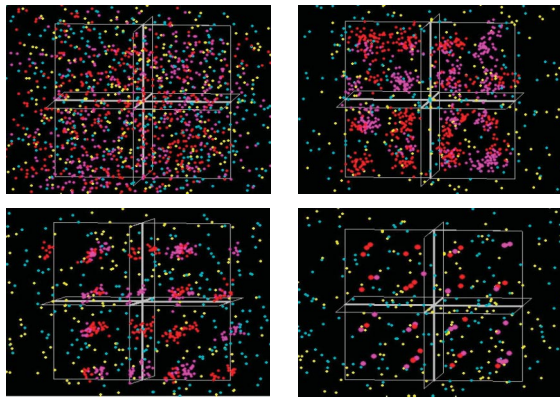
(band structure) with increased concentration at distances smaller than $0.5a_B$. Finally, we computed the relative distance fluctuations of the holes as a function of mass ratio at $T_e = 0.64$ and $r_{se} = 0.63$. They show a strong increase around $M = 80$–100 typical for a solid-liquid transition (not displayed).

Phase diagram.—We now construct the generic phase diagram of the TCP which applies to all the different Coulomb crystals; see Fig. 3. Consider first the case of a hole crystal in semiconductors which is embedded into a dense Fermi gas of electrons. The holes behave classically above the black dotted line and quantum-mechanically below (this line is given by $n_h \Lambda_h^3 = 1$, where $\Lambda_h = h/\sqrt{2\pi m_h k_B T_h}$ is the thermal hole de Broglie wavelength). The e-h bound state phase is shown in the left part and contains excitons and biexcitons and, eventually at low temperature, a Bose liquid, superfluid, or an excitonic insulator [17]. On leaving this phase across its boundary [given by the line $r_{se}(T_e) = r_s^{Mott}(T_e)$], the fraction of bound states rapidly vanishes in favor of unbound e-h pairs with the holes showing liquidlike behavior. Upon further compression (at temperatures $T_e < T^*$), the hole liquid crystallizes, provided $M \gtrsim M^{cr}$. At the density $n^{(2)}$, quantum melting of the crystal is observed (vertical long-dashed green line). The entire hole Coulomb crystal phase for $M = 200$ is marked by the full red line in Fig. 3.

Now, how is the hole crystal in semiconductors related to the Coulomb crystals in classical and astrophysical plasmas mentioned in the introduction? To answer this question, we investigate the dependence of the stability of the crystal phase on the three asymmetry parameters. When M is reduced, the crystal phase shrinks (see the red short-dashed line corresponding to $M = 100$) until, for $M = M^{cr}$, it vanishes. Vice versa, when M becomes larger, both maximum density and temperature at which crystal-

FIG. 1 (color). Snapshots of an e-h plasma at $T_e = 0.096$, and $r_{se} = 0.63$. Clouds of blue (yellow) dots mark the fully delocalized electrons with spin up (down); clouds of red (pink) dots denote holes with spin up (down). Top left (right): $M = 5$ (50), bottom left (right): $M = 100$ (800).
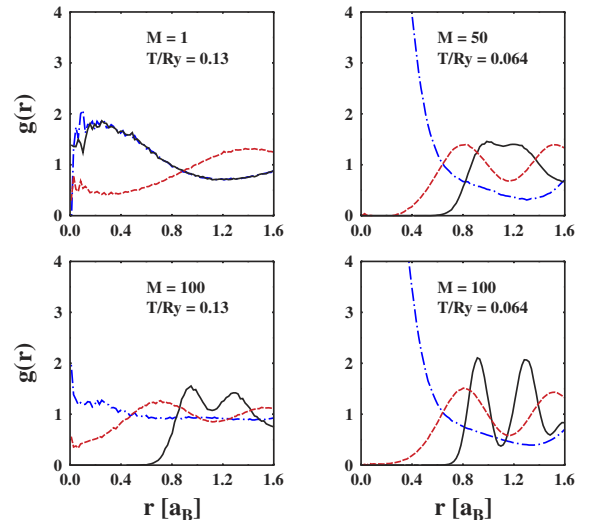

FIG. 2 (color online). e-e (blue, dashed-dotted line), h-h (black, solid line), and e-h (red, dotted line) pair distribution functions for different mass ratios and temperatures.
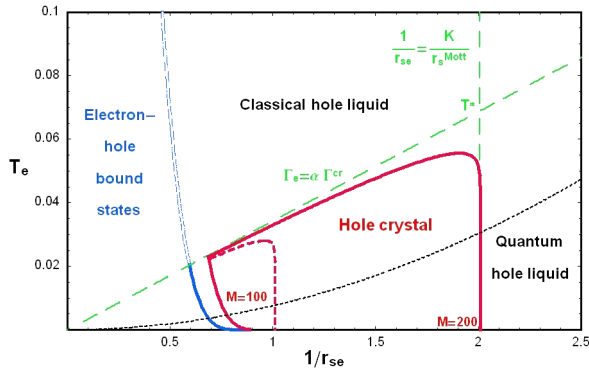
FIG. 3 (color online). Phase diagram of a two-component plasma in the plane of dimensionless electron temperature T_e and density parameter $1/r_{se}$. The boundary of the Coulomb bound state phase is given by $r_s^{\text{Mott}}(T_e)$. Above (below) the dotted black line, holes are classical (degenerate). The red full (dashed) line is the boundary of the hole crystal for $\Theta = Z = 1$ and $M = 200$ ($M = 100$) with the asymptotics given by Eqs. (1) and (5) (green long-dashed lines). $\alpha = 1/(Z^2/\Theta)$.

lization is possible increase according to Eqs. (5) and (6). While in semiconductors in quasiequilibrium, M is the only parameter which can be varied from one material to another, the diversity of ionic plasmas, on the other hand, offers additionally control of the charge and temperature ratios Z and Θ in very broad ranges. By increasing M, Z, and Θ, the crystal phase extends further towards higher density and temperature, covering an ever increasing part of the temperature-density plane (with the exception of the bound state phase). Eventually, this crystal phase will overlap with the known classical and astrophysical Coulomb crystals at low and high densities, respectively. Thus, indeed, the phase diagram in Fig. 3 applies to all Coulomb crystals in two-component plasmas of electrons and pointlike ions, independently of their physical origin. Of course, in different systems specific additional factors may exist. For example, phase separation or non-Coulombic bound states will modify the boundary of the bound state phase and the value of $n^{(1)}$, whereas band structure effects or extended ionic cores can modify the high-density behavior [15]. Finally, while our analytical results for the crystal phase are obtained neglecting e-h correlations (which is justified by the large mass ratio M), the simulations indicate that the electrons have a stabilizing influence, increasing the maximum temperature beyond T^*. These effects are beyond the present investigation and will be discussed elsewhere.

In summary, one of the most fundamental collective properties of matter, Coulomb crystallization, has been extended from one-component plasmas to the case of neutral systems with two oppositely charged components. Our analysis provides a common view and general quantitative bounds on the critical parameters for the existence of Coulomb crystals in a large variety of TCP, including dwarf stars, laser-cooled expanding plasmas, dusty plasmas, and semiconductors. The critical parameters depend on the combined mass, charge, and temperature asymmetry between the heavy and light components. Crystallization of protons and of holes in semiconductors is predicted. Hole crystals should exist in materials with a mass ratio of about 80 [21] and might be observable in rare earth semiconductors in neutron scattering experiments. These hole crystals could serve as a valuable testing ground for quantum TCP crystals, in general, and for ion crystals in exotic stellar objects, in particular.

[1] E. Wigner, Phys. Rev. **46,** 1002 (1934).
[2] C. C. Grimes and G. Adams, Phys. Rev. Lett. **42,** 795 (1979).
[3] See A. V. Filinov, M. Bonitz, and Yu. E. Lozovik, Phys. Rev. Lett. **86,** 3851 (2001), and references therein.
[4] See, e.g., W. M. Itano *et al.*, Science **279,** 686 (1998).
[5] T. Schätz, U. Schramm, and D. Habs, Nature (London) **412,** 717 (2001).
[6] G. J. Kalman, P. Hartmann, Z. Donko, and M. Rosenberg, Phys. Rev. Lett. **92,** 065001 (2004).
[7] H. DeWitt *et al.*, Contrib. Plasma Phys. **41,** 251 (2001).
[8] D. M. Ceperley and B. J. Alder, Phys. Rev. Lett. **45,** 566 (1980).
[9] H. Thomas *et al.*, Phys. Rev. Lett. **73,** 652 (1994); Y. Hayashi and K. Tachibana, Jpn. J. Appl. Phys. **33,** L804 (1994).
[10] O. Arp, D. Block, A. Piel, and A. Melzer, Phys. Rev. Lett. **93,** 165004 (2004).
[11] T. Pohl, T. Pattard, and J. M. Rost, Phys. Rev. Lett. **92,** 155003 (2004).
[12] For details, see, e.g., L. Segretain, Astron. Astrophys. **310,** 485 (1996).
[13] B. I. Halperin and T. M. Rice, Rev. Mod. Phys. **40,** 755 (1968).
[14] We distinguish plasma crystals from ionic crystals (such as NaCl) and metals, the properties of which are essentially dictated by the electronic structure of the ionic cores.
[15] For ions with an internal structure, the upper density limit may deviate from Eq. (5), which refers to point charges, as their compression may lead to structural transitions rather than melting.
[16] This is close to the estimate of 100 for CuCl given by A. A. Abrikosov, J. Less-Common Met. **62,** 451 (1978).
[17] B. Bucher, P. Steiner, and P. Wachter, Phys. Rev. Lett. **67,** 2717 (1991); P. Wachter, B. Bucher, and J. Malar, Phys. Rev. B **69,** 094502 (2004).
[18] V. S. Filinov, M. Bonitz, W. Ebeling, and V. E. Fortov, Plasma Phys. Controlled Fusion **43,** 743 (2001).
[19] V. S. Filinov *et al.*, J. Phys. A **36,** 6069 (2003).
[20] H. Fehske, V. Filinov, M. Bonitz, and V. E. Fortov, J. Phys.: Conf. Ser. **11,** 139 (2005).
[21] In two dimensions, Eq. (4) yields $M^{\text{cr}} \approx 60$, where $r_{s2d}^{\text{cr}} \approx 74$ and $r_{s2d}^{\text{Mott}} = 1.2$ have been used (r_{s2d} refers to the 2d exciton Bohr radius), but r_{s2d}^{Mott} still needs to be verified by simulations.